

Spectroscopic Studies of the S_0 – S_1 Transition of Substituted 1-Aminonaphthalenes in a Supersonic Jet

Françoise Lahmani,^{*,†} Anne Zehnacker-Rentien,[†] Laurent H. Coudert,[†] and
Klaas A. Zachariasse[‡]

Laboratoire de Photophysique Moléculaire du CNRS, Bat. 210, Université de Paris-Sud, F-91405 Orsay Cedex, France, and Max-Planck-Institut für biophysikalische Chemie, Spektroskopie und Photochemische Kinetik, 37070 Göttingen, Germany

Received: March 18, 2003; In Final Form: June 9, 2003

The spectroscopic properties of a series of 1-aminonaphthalenes were examined in the isolated gas phase by means of laser-induced fluorescence combined with supersonic beam techniques. The aminonaphthalenes differ with respect to the size of the amino group, 1AN (NH_2), 1MAN (NHCH_3), 1DMAN ($\text{N}(\text{CH}_3)_2$), or the presence of a second substituent in the 4-position: 4MDMAN (CH_3) and 4CIDMAN (Cl). Whereas the fluorescence excitation spectra of 1AN and 1MAN show an intense 0–0 transition and a well-resolved vibrational pattern, that of the *N,N*-dimethylamino derivative 1DMAN displays a particularly complex structure, with a very weak origin and a sudden collapse of intensity at excitation energies above 1000 cm^{-1} . A long low-frequency vibrational progression, which has been assigned to the torsional mode of the $\text{N}(\text{CH}_3)_2$ around the C–N bond, clearly appears in the spectra of the 4-substituted derivatives. DFT calculations of the ground-state structure of 1DMAN and 4CIDMAN show that the dimethylamino group is twisted by 49.7° relative to the aromatic plane. An analysis of the Franck–Condon distribution along the torsional progression for 4CIDMAN indicates a decrease of the dimethylamino twist angle in S_1 by about 20° . The energy threshold for the drop in fluorescence intensity, depending on the nature of the substituent in the 4-position (1200 cm^{-1} for 4MDMAN, 700 cm^{-1} for 4CIDMAN), indicates the presence of an efficient internal conversion process, similar to what has previously been observed in solution. Complexation of 1DMAN with acetonitrile reduces the internal conversion efficiency, as can be deduced from the enhanced fluorescence intensity as well as from the lengthening of the fluorescence decay time. The collapse of the FES spectrum of the 1DMAN/ CH_3CN complex (1:1) occurs at a significantly higher excess energy (1500 cm^{-1}) than in the case of bare 1DMAN.

Introduction

The UV spectrum of naphthalene presents two closely lying π – π^* S_0 – S_1 , and S_0 – S_2 electronic transitions, polarized along the long and short molecular axis, respectively. These transitions are described as excitations to so-called L_b (S_1) and L_a (S_2) states.¹ In the nonsubstituted naphthalene molecule, the first S_0 – S_1 transition is characterized by a very small oscillator strength due to almost destructive interference between two single-electron configurations and becomes vibronically allowed via Herzberg–Teller coupling to the second strongly allowed S_0 – S_2 transition.² The introduction of a substituent substantially changes the spectroscopic properties of the naphthalene molecule. First, the S_0 – S_1 transition gains intensity, as it is no longer forbidden because of symmetry breaking. Second, depending both on the chemical nature of the substituent and on its position in the naphthalene ring, the relative energy and the coupling of the S_2 and S_1 states (L_a and L_b in the parent molecule) are modified.^{3,4} The substitution at the 1-position is known^{3,4} to induce a large red shift of the L_a band of naphthalene, in contrast to a relatively small red shift of the L_b band, which reduces the

energy gap between the S_1 and S_2 states. The effect of introducing an electron-donating amino group in the 1-position of naphthalene is particularly dramatic in this respect. The two lowest π – π^* electronic states of 1-aminonaphthalene derivatives become very close in energy and hence a single broad absorption band is observed in solution, consisting of the two overlapping perturbed $S_2(L_a)$ and $S_1(L_b)$ bands. In the gas phase, the first electronic transition of 1-aminonaphthalene (1AN) has been shown by high-resolution spectroscopy to be short axis polarized,⁵ in contrast to other 1-substituted naphthalenes,⁶ demonstrating unambiguously an inversion of the $S_2(L_a)$ and $S_1(L_b)$ states in this molecule. Another important spectroscopic characteristic induced by the presence of the amino group in 1AN is related to the geometry of this group relative to the naphthalene plane and its modification upon excitation. Whereas the NH_2 group of 1AN is twisted by 20° and has an inversion angle of about 47° in the S_0 state, it becomes almost coplanar with the naphthalene ring in S_1 .⁵ This planarization of the amino group is a manifestation of the enlarged electron delocalization in the S_1 state of 1AN, caused by the conjugation of the lone pair of the *N* atom with the π electrons of the naphthalene moiety. It is also important to stress that this increased delocalization in the planar S_1 state confers a significant charge-transfer character to the lowest S_0 – S_1 transition, directed from the NH_2 substituent to the aromatic ring.

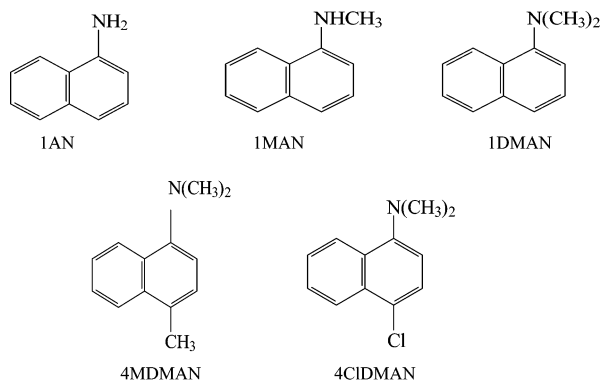
* To whom correspondence should be addressed. E-mail: francoise.lahmani@ppm.u-psud.fr.

[†] Université de Paris-Sud.

[‡] Max-Planck-Institut für biophysikalische Chemie, Spektroskopie und Photochemische Kinetik.

The photophysical properties of 1-aminonaphthalene derivatives in solution have been the subject of considerable interest.⁷ The replacement of NH₂ in 1AN by a dialkylamino group, giving 1-(dimethylamino)naphthalene (IDMAN), gives rise to the appearance of an unexpectedly fast nonradiative decay in a nonpolar medium, which process originates from the equilibrated S₁ state. This fast decay channel was first observed by Meech et al. and manifests itself by a low fluorescence quantum yield and a correspondingly short fluorescence decay time.⁷ Further detailed studies^{8–11} on the effect of temperature and of solvent polarity on the fluorescence and triplet quantum yields, together with fluorescence lifetime measurements in a series of 1-aminonaphthalene derivatives, have shown that a thermally activated internal conversion is responsible for the excited-state behavior. It was concluded that the internal conversion process depends on the extent of the amino twist angle in S₀ and its change upon excitation.^{8–11} The energy barrier for internal conversion was found to increase with solvent polarity. These effects have been explained on the basis of a model involving the vibronic coupling between the proximate S₁ and S₂ states along the twist angle coordinate, which allows the internal conversion process to take place through a conical intersection with the S₀ state.^{10,11} When the solvent polarity increases, the excited state S₁ is preferentially stabilized, as it has a larger charge-transfer character than the S₂ state. Thereby, the energy gap $\Delta E(S_1, S_2)$ becomes larger, which results in a decrease of the electronic coupling between the two states. As a consequence, the shape of the potential energy surface (PES) of S₁ is altered and the conical intersection with the S₀ state is shifted to higher energy.

Our objective in this investigation is to compare the spectroscopic properties of the 1-aminonaphthalene derivatives pictured below, using laser-induced fluorescence (LIF) techniques combined with supersonic jet-cooling, to bring new insights on the factors that influence the photophysics of the isolated molecules. Because the preparation of cold isolated gas-phase species in a supersonic expansion removes much of the spectral congestion inherent to condensed phases and prevents collisional relaxation, one expects from this approach a better knowledge of the excited-state potential energy surfaces of these systems. The role of the twist angle around the C–N bond of the aminonaphthalenes, resulting from the interaction between the amino substituent and the hydrogen atom in the 8-position of the naphthalene moiety, was examined by studying the influence of methyl substitution in the amino group on the spectroscopic behavior of the three molecules 1AN, 1-(methyl-



amino)naphthalene (1MAN), and 1DMAN. Further experiments were carried out with 4-methyl-1-(dimethylamino)naphthalene (4MDMAN) and 4-chloro-1-(dimethylamino)naphthalene (4CIDMAN), to study the effect of a second substituent with electron donor (CH₃) or acceptor (Cl) character on their photophysics.

Such an effect has been observed with these molecules in solution.¹¹ Finally, the influence of complexation of jet-cooled 1DMAN with CH₃CN was investigated, to obtain information at the microscopic level on the stabilization of the excited state of this molecule by a strongly polar solvent.

Experimental and Theoretical Methods

The experimental setup for the present jet experiments is the same as that used previously.¹² Briefly, it consists of a continuous supersonic expansion of helium (2–3 atm backing pressure) through a 200 μ m pinhole. The compounds under study are slightly heated just before the expansion to obtain sufficient vapor pressure and they are excited by a frequency-doubled dye laser (LDS 698) pumped by the second harmonic of a YAG laser (Quantel). Fluorescence was observed at the right angle of the jet and laser beam axes through a (Schott WG 365) cutoff filter and focused by means of collimating optics through a slit onto a Hamamatsu R2059 photomultiplier. For dispersed fluorescence experiments, the emitted light was analyzed either by a 60 cm Jobin–Yvon monochromator (1200 grooves/mm holographic grating, $\Delta\nu = 30 \text{ cm}^{-1}$) or at low resolution by a 25 cm Jobin–Yvon monochromator (300 grooves/mm grating, $\Delta\nu = 200 \text{ cm}^{-1}$). The signal was monitored by a Lecroy 9400 oscilloscope and processed with a LabVIEW-based computer program. The fluorescence decays were measured by employing a 9400 Lecroy oscilloscope working in the sweeping mode. The temporal resolution of the laser is 8 ns and the photomultiplier rise time less than 2 ns. The experimental lifetimes were determined from the fitting of the experimental decay curves with the iterative convolution of the time profile of the scattered light from the laser with an exponential decay.

1AN and 1DMAN were purchased from Aldrich. 1MAN, 4MDMAN, and 4CIDMAN were synthesized as described previously.¹¹

Ab initio calculations of the structure of 1DMAN and 4CIDMAN were carried out at the DFT level, using the Gaussian 98 software package.¹³ The energy optimization and the calculation of the harmonic frequencies were performed with the B3LYP hybrid HF density functional and the 6-31G** basis set provided in the Gaussian package.

Results

Fluorescence Excitation and Dispersed Emission Spectra of 1AN, 1MAN, and 1DMAN. The fluorescence excitation spectra (FES) of 1AN, 1MAN, and 1DMAN are shown in Figure 1. The FES of 1AN is similar to the one reported previously⁵ and exhibits a well-resolved vibrational pattern with a strong 0–0 transition at 30 044 cm^{-1} . The FES spectrum of 1MAN likewise consists of sharp features. Its origin, located at 29 437 cm^{-1} , is red-shifted by 607 cm^{-1} relative to that of 1AN. The main vibrational bands observed within $\sim 1000 \text{ cm}^{-1}$ above the origin for both compounds are collected in Table 1. The dispersed fluorescence spectrum of 1AN has already been reported by Berden et al.⁵ and only that of 1MAN will be depicted here (Figure 2). This spectrum shows a resonant type emission superimposed on a background of increasing intensity towards the red. The maximum of emission recorded at low resolution (spectrum not shown), is located at about 1700 cm^{-1} from the transition origin. The ground-state vibrational frequencies appearing in the fluorescence spectra resulting from the 0⁰ level excitation of 1AN and 1MAN are also listed in Table 1.

Different from 1AN and 1MAN, the FES of 1DMAN presents a peculiar shape (see Figure 1): a series of dense features

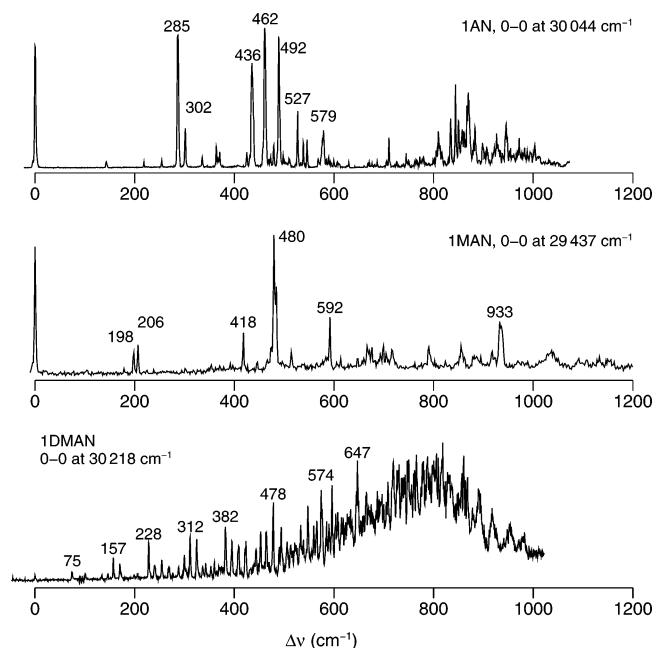


Figure 1. Fluorescence excitation spectra of (a) 1-aminonaphthalene (IAN), (b) 1-(methylamino)naphthalene (IMAN), and (c) 1-(dimethylamino)naphthalene (1DMAN). The energy scale is relative to the 0-0 transition of each molecule.

TABLE 1: Prominent Vibrational Bands Observed in the Excitation and Dispersed Fluorescence Spectra of IAN and IMAN and Corresponding Decay Times^a

IAN			IMAN		
$\Delta\nu$ (S ₁) (cm ⁻¹)	$\Delta\nu$ (S ₀) (cm ⁻¹)	τ (ns)	$\Delta\nu$ (S ₁) (cm ⁻¹)	$\Delta\nu$ (S ₀) (cm ⁻¹)	τ (ns)
0		14 ± 1	0	202	13 ± 1
285	262	18 ± 1	198		10 ± 1
300		13 ± 1	206		11 ± 1
436		11 ± 1	418	383	12 ± 1
462	470	14 ± 1			
492		17 ± 1	480	484	11 ± 1
531		11 ± 1	484		11 ± 1
580			592		11 ± 1
723	734		700		
828			790	807	
850			850	857	
860					
	943			971	
	1032			1370	
				1582	

^a $\Delta\nu$ is measured with respect to the 0-0 transitions of IAN and IMAN at 30044 and 29437 cm⁻¹.

develops continuously over 1000 cm⁻¹ with increasing intensity and congestion. Because of the low intensity of the lines at the onset of the spectrum, the transition origin is difficult to determine. The first very weak feature appears at 30 218 cm⁻¹ and the intensity distribution peaks at about 31 000 cm⁻¹. Above 800 cm⁻¹ excess energy, the intensity starts to decrease, ending by a group of broad bands separated by ~30 cm⁻¹. Although the intensity drop is quite sharp, there is still a weak and continuous background signal at excess energies larger than 1000 cm⁻¹. In contrast with IAN and IMAN, the strongly displaced Franck-Condon contour observed in this spectrum indicates that a large change in molecular geometry takes place in the excited state as compared to that of the ground state. A recent study on jet-cooled 4-(diisopropylamino)benzotrile (DIABN)¹⁴ has shown that the FES spectrum of this molecule

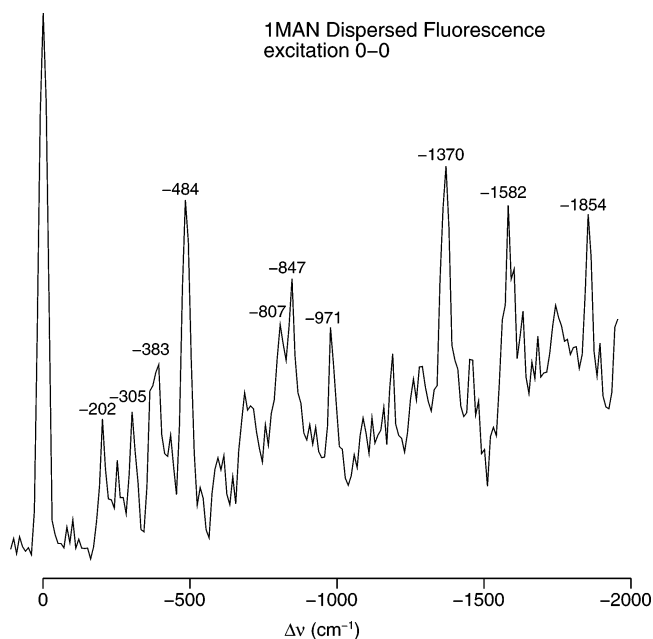


Figure 2. High-energy part of the dispersed fluorescence of 1-(methylamino)naphthalene (IMAN) excited in the 0-0 transition at 29 347 cm⁻¹ ($\Delta\nu = 30$ cm⁻¹).

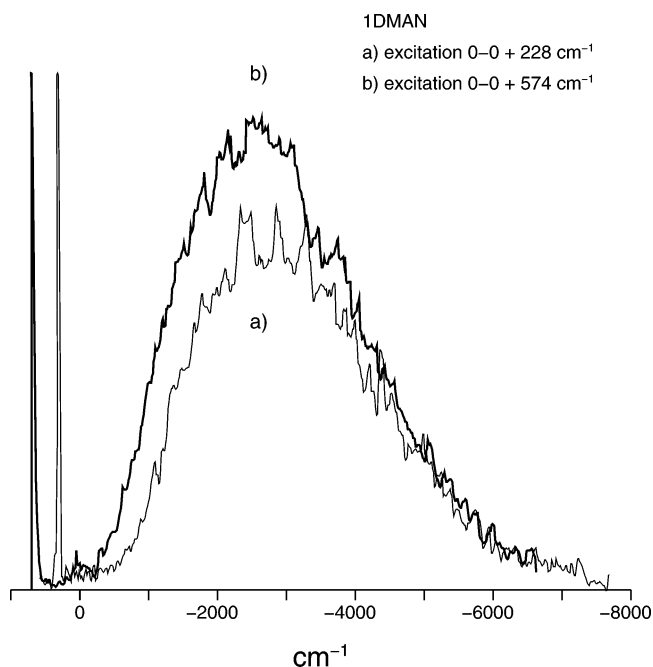


Figure 3. Dispersed fluorescence spectrum of 1-(dimethylamino)naphthalene (1DMAN) recorded under broad spectral resolution ($\Delta\nu = 200$ cm⁻¹). The energy scale is relative to the 0-0 transition at 30 218 cm⁻¹. The excitation is set on the narrow features, at (a) 0-0 + 228 cm⁻¹ and (b) 0-0 + 574 cm⁻¹.

undergoes a similar sudden decrease in its intensity at an excess excitation energy of 800 cm⁻¹.

The very weak intensity of the origin bands of 1DMAN (Figure 1) prevents the study of the dispersed emission spectra for excitation of the 0⁰ level. Therefore, the fluorescence has been recorded at low resolution ($\Delta\nu = 200$ cm⁻¹) for the excitation of the strong bands at 218 and 574 cm⁻¹ above the 0-0 transition. The onset of the emission spectra shown in Figure 3 occurs close to the origin of the transition and its maximum peaks at about 2700 cm⁻¹ from it ($\lambda_{\text{max}} = 363$ nm). This behavior is typical for an extended intramolecular vibrational redistribution in the S₁ of large molecules and indicates

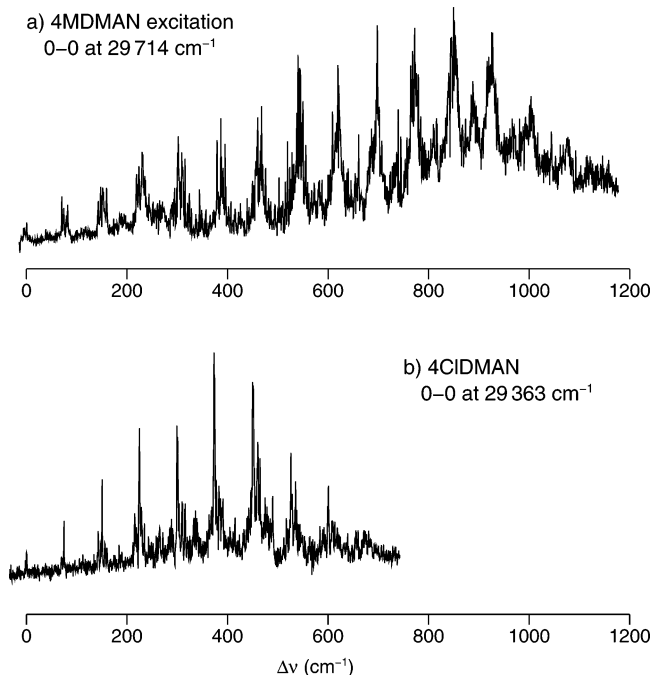


Figure 4. Fluorescence excitation spectrum of (a) 4-methyl-1-(dimethylamino)naphthalene (4MDMAN) and (b) 4-chloro-1-(dimethylamino)naphthalene (4CIDMAN).

strongly displaced ground- and excited-state potential energy surfaces. For 1MAN the shift is only 1700 cm⁻¹, as observed from the emission recorded under similar broad band conditions. This difference in the Franck–Condon envelope of the dispersed fluorescence supports the conclusion that for 1DMAN a large difference exists between S₁ and S₀ equilibrium geometry, as was already suggested by the excitation spectrum. From the large Stokes shift $\Delta\nu(\text{St})$ (6800 cm⁻¹) between the maxima of the absorption and fluorescence spectra of 1DMAN in *n*-hexane at 25 °C as compared with $\Delta\nu(\text{St})$ for 1AN (3980 cm⁻¹) and 1MAN (4920 cm⁻¹), it was likewise concluded that the change of the amino twist angle of 1DMAN is considerably larger than that of 1AN and 1MAN.¹⁰

The fluorescence decay times obtained by pumping selected vibrational levels of 1AN and 1MAN are reported in Table 1. In the case of 1DMAN, the decay times are within the width of the excitation laser pulse (8 ns).

Effect of Substitution in the 4-Position of 1DMAN on the Excitation Spectra. The FES of 4MDMAN and 4CIDMAN are displayed in Figure 4. These spectra of the two molecules look similar and also bear a resemblance to that of 1DMAN (Figure 1): the 0–0 transition is very weak and an increase of the overall intensity as well as of the congestion is observed as a function of excess energy. Both spectra have undergone a red-shift with respect to that of 1DMAN, because the first weak bands taken as the origin of the S₀–S₁ transitions occur at 29 714 and 29 363 cm⁻¹, respectively, instead of 30 218 cm⁻¹, as found for 1DMAN. A second important difference with 1DMAN is immediately apparent in these spectra. Whereas the complexity and the band congestion prevent the assignment of a low-frequency progression in the case of 1DMAN, the spectrum of 4MDMAN as well as of 4CIDMAN is dominated by a long progression involving regular energy intervals of ~ 75 cm⁻¹. In 4MDMAN, the observed 14 members in the progression consist of a group of close features that become more dense and broad at higher energies. Above 1200 cm⁻¹ excess energy, the overall intensity decreases, being replaced by a less intense continuum. The progression observed in 4CIDMAN is shorter:

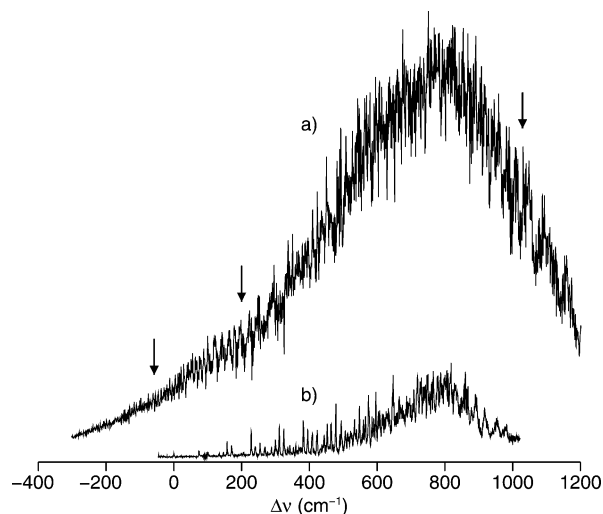


Figure 5. Fluorescence excitation spectrum obtained by adding acetonitrile to jet-cooled 1-(dimethylamino)naphthalene (1DMAN) (a) as compared to that of the bare molecule (b), from Figure 1. The arrows indicate the excitation energy at which lifetimes have been measured.

it consists of nine members and extends only over 700 cm⁻¹. The intensity distribution peaks on the sixth feature and decreases very rapidly above 700 cm⁻¹ excess energy. It can be seen from Figure 4 that each member of the progression with 4CIDMAN is less congested than in the case of 4MDMAN.

Effect of Complexation of 1DMAN with Acetonitrile. The FES of 1DMAN in the presence of acetonitrile is shown in Figure 5. After addition of CH₃CN, the excitation spectrum undergoes a strong enhancement of its intensity and displays a broad and continuous band, without any of the fine structure observed in the isolated molecule in Figure 1. The onset of this spectrum is red-shifted by ~ 300 cm⁻¹ with respect to the 0–0 transition of bare 1DMAN and its intensity peaks at about the same energy (31 000 cm⁻¹), as observed for the uncomplexed molecule. Similar to the bare molecule, however, its intensity drops quite rapidly, but at a higher excess energy (~ 1500 cm⁻¹) above the onset. The overall intensity of the signal depends linearly on the partial CH₃CN pressure, which shows that it involves mainly a 1:1 complex. Besides the increase in intensity, which indicates a large fluorescence quantum yield of the complex with acetonitrile, it is to be noted that its fluorescence decay time is longer than that of isolated 1DMAN ($\tau = 20 \pm 1$ ns vs $\tau < 8$ ns). The decay time of the 1DMAN/CH₃CN complex measured at several excitation wavelengths across the spectrum (see Figure 5) was shown not to depend on the excess energy in the excited state with a constant value for τ of 20 ns.

Discussion

The examination of the spectroscopic properties of the 1-(dimethylamino)naphthalenes 1DMAN, 4MDMAN, and 4CIDMAN in the isolated gas phase investigated here clearly shows that they are similar to the unusual behavior of these compounds already observed in solution.^{8–11} Three questions will be addressed in the following discussion: (a) What is the molecular nature of the excited states observed in the experiments? (b) How does the twist of the dimethylamino group affect the electronic spectroscopy of the molecules? (c) What can be learned concerning the mechanism of the energy dependent nonradiative process occurring in the (dimethylamino)naphthalenes?

Characteristics of the S₀–S₁ Transitions in the Isolated Aminonaphthalenes. The energy as well as the nature of the

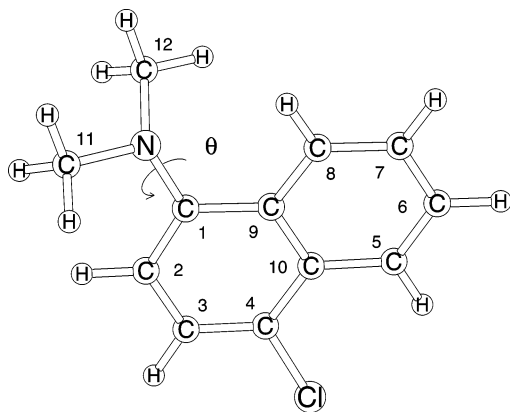


Figure 6. Calculated structure of 4-chloro-1-(dimethylamino)naphthalene (4CIDMAN) in the electronic ground state S_0 , showing the torsional angle θ of the $N(CH_3)_2$ substituent relative to the plane of the chloronaphthalene moiety. The twist angle θ is equal to 90° when the molecule has a plane of symmetry, the $N(CH_3)_2$ group pointing away from the naphthalene plane.

S_0 – S_1 transition of the 1-aminonaphthalenes studied here can be explained by the combination of two opposing effects. First, the electron donating character of the lone pair electrons of the nitrogen atom enlarges the conjugation of the π electron system, thereby decreasing the energy of the transition. Second, the steric hindrance exerted on the amino group by the H8 atom of the aromatic frame of the 1-aminonaphthalenes (see Figure 6 below) induces a twist around the C–N bond, which reduces the interaction of the electron donating amino group with the naphthalene nucleus.

The energy of the S_1 state of the jet-cooled isolated 1AN and 1MAN molecules in the gas phase (Figure 1) is equal to 30 044 and 29 437 cm^{-1} , respectively, and is to be compared with this energy deduced from the intersection of the absorption and emission spectra in *n*-hexane solution.^{10,11} In such a nonpolar solvent at room temperature, the S_1 transition energy of both 1AN and 1MAN is about 1000 cm^{-1} lower than in the jet-cooled gas phase. This means that the relative red shift of the S_0 – S_1 transition of 1MAN with respect to that of 1AN is similar in the gas phase and in solution ($\sim -600 \text{ cm}^{-1}$ vs -770 cm^{-1}).

The second *N*-methyl group in 1DMAN induces a blue shift of the transition origin relative to 1MAN (Figure 1). Under the assumption that the first observed peak in the FES spectrum of 1DMAN corresponds to the 0–0 transition, the shift ($+781 \text{ cm}^{-1}$) is similar to what has been observed in solution ($+630 \text{ cm}^{-1}$ in *n*-hexane at 25 $^\circ\text{C}$).¹⁰ As emphasized before,^{8,10,11} this effect is a consequence of the twist angle of the $N(CH_3)_2$ group in 1DMAN, which is larger than that of the NH_2 substituent of 1AN or the NHCH_3 group in 1MAN, due to the repulsive interaction exerted by the hydrogen atom in the 8-position of the naphthalene ring (peri effect); see above.¹⁵ The blue shift of the first electronic transition observed in 1DMAN relative to 1MAN and 1AN is again explained by the decrease of the electronic coupling between the nonbonding electrons of the N atom of the amino group and the π electrons of the naphthalene ring.

For 4MDMAN and 4CIDMAN, the substitution in the 4-position leads to a decrease of the S_0 – S_1 transition energy relative to 1DMAN of 504 and 855 cm^{-1} in the jet-cooled gas phase (see Figures 1 and 4) and of 800 and 990 cm^{-1} in *n*-hexane solution at 25 $^\circ\text{C}$,¹¹ respectively. These shifts are caused by the presence of the methyl and Cl substituents, because in 4MDMAN and 4CIDMAN the same conformation (amino twist) of the $N(CH_3)_2$ group as in 1DMAN is to be

expected; see below. The red shifts observed for these 4-substituted compounds are comparable to those induced by methyl and Cl substitution in the 1-position on the energy of the L_a state of the parent naphthalene molecule: spectral shifts $\Delta\nu$ of 780 and 950 cm^{-1} , respectively, are observed in hydrocarbon solutions, as compared with 290 and 415 cm^{-1} for the L_b state.¹⁶

The symmetry of the S_1 state of 1AN in the gas phase has been deduced from rotationally resolved spectroscopy,⁵ which gives the direction of the transition moment with respect to the inertial axes of the molecule. Such high-resolution experiments have shown that the S_0 – S_1 transition is polarized along the short axis of the naphthalene frame. The first excited state of 1AN has thus similarities with the L_a state of naphthalene. It has also been shown that the rotational contour of the band varies significantly with vibrational excitation, and this effect may indicate that vibronic mixing takes place between the closely lying excited states with predominant $L_a(S_1)$ and $L_b(S_2)$ parentage. On the basis of the similarity of the spectral properties of 1MAN and 1AN, it is concluded that also in the case of 1MAN the lowest excited state has L_a character.

The situation is less clear for the 1DMAN derivatives. Because of the decrease in the coupling between the n orbital of the dimethylamino group and the π orbitals of naphthalene, caused by the twist of the $N(CH_3)_2$ substituent, the energy of the L_a state is expected to increase and the absorption bands of the two lowest excited states (L_a and L_b) may thus overlap in the Franck–Condon region. This could explain the complexity of the excitation spectrum in the region of the vertical transition. One can, as a consequence, not make a decision on the nature of the S_1 state in isolated 1DMAN on the basis of an examination of the spectroscopic data alone. A comparison with experiments in solution nevertheless shows that the redistributed emission observed in the gas phase corresponds to that originating from the “equilibrated S_1 state” measured in solution. This equilibrated state has been assigned to the L_a state on the basis of its large dipole moment obtained from fluorescence solvatochromism measurements and *ab initio* calculations.⁹

The L_a state of naphthalene derivatives is known to be strongly allowed and this property should manifest itself by a large radiative rate constant and hence by a shortening of lifetimes as compared with naphthalene derivatives in which the lowest excited state is the L_b state.¹⁷ The fluorescence decays of 1AN and 1MAN have been measured for excitation of different vibronic levels and are found to have values in the range 11–18 ns for 1AN and between 10 and 12 ns for 1MAN. These fluorescence lifetimes are substantially shorter than those determined for other jet-cooled 1-substituted naphthalenes, having values from 353 ns for 1-methylnaphthalene to 110 ns for 1-fluoronaphthalene¹⁸ and 61 ns for 1-naphthol.¹⁹

The fluorescence decay time τ_F can be expressed as

$$\tau_F = 1/(k_R + k_{NR}) = \Phi_F/k_R \quad (1)$$

where k_R and k_{NR} are the rate constants for the radiative and nonradiative decay processes and Φ_F is the fluorescence quantum yield. The radiative rate constant k_R cannot directly be obtained from the decay time τ_F , as the fluorescence quantum yield Φ_F necessary for its determination (eq 1) is not easily accessible from jet experiments. Nevertheless, the relatively short fluorescence decay times obtained for the strongly fluorescent jet-cooled 1AN and 1MAN suggest correspondingly large radiative rates k_R , which are consistent with the assignment of S_1 to a state of L_a parentage. In the case of 1DMAN, however, the fluorescence decay time was too short to give reliable data with our experimental setup. Because the radiative rate constant

k_R of 1DMAN is not expected to differ strongly from those of 1AN and 1MAN, as observed in *n*-hexane solution at 25 °C ($k_R = 6.6, 7.4,$ and $8.3 \times 10^7 \text{ s}^{-1}$ respectively for 1AN, 1MAN, and 1DMAN¹⁰), this significant shortening of the fluorescence decay times indicates the presence of a fast nonradiative process in this molecule.

An important property of the 1-aminonaphthalenes discussed here, is the change in the geometry of the amino substituent in the excited state. The conformation of the amino group in the ground state involves two angles: the twist angle around the C–N bond and the pyramidal angle of the NR₂ substituent with respect to the aromatic plane as described below. Due to the increased electronic delocalization in the S₁ state, the C–N bond gains double bond character, which implies a more planar geometry of the amino group in the excited state and thus a reduced pyramidal angle and twist angle in S₁ as compared with S₀.

The planarization of the amino group upon excitation of an aminonaphthalene has recently been deduced from the analysis of the rotationally resolved excitation spectra of 1AN.⁵ The NH₂ group is twisted by 20° in S₀ whereas the molecule is practically planar in S₁.⁵ The normal mode associated with the NH₂ torsion has been assigned to the vibration observed at 262 cm⁻¹ in S₀ and 282 cm⁻¹ in S₁. The comparison between the excitation and dispersed fluorescence spectra of 1AN and 1MAN (Figures 1–3) shows that the twist of the NH(CH₃) group in 1MAN can be assigned to either component of the 198–206 cm⁻¹ doublet band in S₁, which has its counterpart in the band at 202 cm⁻¹ in S₀. The decrease in frequency can be attributed to the change of the reduced mass of 1MAN with respect to 1AN. Further, whereas the first vibronic band at 282 cm⁻¹ has a similar intensity as the 0–0 transition in 1AN, the 198–206 cm⁻¹ bands of 1MAN show a much more reduced intensity with respect to the origin transition. The modest Franck–Condon intensity of this mode in S₁ indicates that 1MAN undergoes upon excitation a smaller change in twist angle than 1AN.

The spectroscopic behavior of 1DMAN and its derivatives 4MDMAN and 4CIDMAN contrasts strongly with that observed for 1AN and 1MAN. The weakness of the 0–0 transition and the increasing Franck–Condon intensity distribution as a function of excitation energy (Figures 1 and 4) reveal that a large change in the molecular conformation takes place upon excitation. Such a displaced Franck–Condon distribution is also evident in the dispersed fluorescence of 1DMAN (Figure 3): as noted before, 1DMAN emission exhibits a larger Stokes shift than 1MAN. Because the coordinate most affected by excitation is expected to be the twist angle of the amino group of 1DMAN, due to its much larger ground-state value as compared to that of 1AN and 1MAN, we can safely attribute the global Franck–Condon contour of the excitation band to the change from the substantial amino twist of 1DMAN in the ground state toward a more planar geometry in S₁.

Whereas for 1DMAN the low-frequency progressions are difficult to extract from the FES spectrum due to its complexity (Figure 1), the spectra of the 4-substituted derivatives of 1DMAN (Figure 4) present a considerably more regular pattern and contain an extended progression developing over 14 quanta for 4MDMAN and 9 quanta for 4CIDMAN, with almost constant spacings of about 75 cm⁻¹. This low-frequency mode, which does not depend on the nature of the additional substituent in the 4-position, can be assigned to the twisting motion of the N(CH₃)₂ substituent around the C–N axis. The long harmonic progression, indicating the presence of a high barrier to internal rotation, is analyzed in the following section.

TABLE 2: Optimized Geometry of 1DMAN and 4CIDMAN in the Ground State^a (B3LYP 6-31G Calculations)**

bond	distance (Å)	angle	(deg)
N–C ₁	1.42	C ₁ –N–C ₁₂	116.5
N–C ₁₁	1.46	C ₁ –N–C ₁₁	114.5
N–C ₁₂	1.46	C ₁₁ –N–C ₁₂	111.4
C ₁ –C ₂	1.38	N–C ₁ –C ₂	122.6
C ₂ –C ₃	1.41	N–C ₁ –C ₉	118.3
C ₃ –C ₄	1.38	C ₁ –C ₂ –C ₃	121
C ₄ –C ₁₀	1.42	C ₂ –C ₃ –C ₄	121
C ₁₀ –C ₅	1.42	C ₃ –C ₄ –C ₁₀	120
C ₅ –C ₆	1.38	C ₄ –C ₁₀ –C ₉	119.5
C ₆ –C ₇	1.41	C ₄ –C ₁₀ –C ₅	121.5
C ₇ –C ₈	1.38	C ₁₀ –C ₅ –C ₆	121
C ₈ –C ₉	1.42	C ₅ –C ₆ –C ₇	120
C ₉ –C ₁	1.44	C ₆ –C ₇ –C ₈	120.5
C ₉ –C ₁₀	1.43	C ₇ –C ₈ –C ₉	118.5
C _{arom} –H	1.09	C ₈ –C ₉ –C ₁₀	119
C _{methyl} –H	1.09	C ₁₀ –C ₉ –C ₁	119
C–Cl ^b	1.76	C ₉ –C ₁ –C ₂	121
		C _{arom} –C _{arom} –H	119
		C ₃ –C ₄ –Cl ^b	118.4
		C ₁₀ –C ₄ –Cl ^b	120
		N–C ₁₁ –H ₁	109
		N–C ₁₁ –H ₂	109
		N–C ₁₁ –H ₃	114
		dihedral angles	
		C ₂ –C ₁ –N–C ₁₁	25.5
		C ₂ –C ₁ –N–C ₁₂	75.3
		C ₁ –N–C ₁₁ –C ₁₂	135
		twist angle (θ) ^c	49.7
		pyramidal angle (Φ) ^c	40

^a Atom numbering is defined in Figure 6. ^b Specific parameter of 4CIDMAN. ^c Twist and pyramidal angles as defined in Figure 7 and text.

Analysis of the Dimethylamino Twist in 1DMAN and 4CIDMAN. The spectra of the three 1-(dimethylamino)-naphthalenes 1DMAN, 4MDMAN, and 4CIDMAN appear to be dominated by vibrational transitions associated with the change in conformation of the dimethylamino group. In this section, calculations on 4CIDMAN are presented. This molecule was chosen because its spectrum best allows a straightforward analysis of the torsion.

Ground-State Geometry and Vibrational Analysis. First, the ground-state molecular geometry of 1DMAN and 4CIDMAN was optimized by using DFT calculations with the B3LYP functional and 6-31G** basis set and the main structural parameters are reported in Table 2. The bond distances and angles are similar for both 1DMAN and 4CIDMAN except the coordinates involving the Cl substituent in the latter case. The computed ab initio geometry of 4CIDMAN is shown in Figure 6. The C₁–N distance is 1.42 Å and the N atom is very slightly displaced out of the aromatic plane by 0.02 Å. In both molecules the dimethylamino group is twisted and bent out of the naphthalene plane. The out-of-plane twist of the dimethylamino substituent around the C₁–N bond is defined as $\theta = (\tau_1 + \tau_2)/2$ where τ_1 and τ_2 are the dihedral angles C₂C₁NC₁₁ and C₉C₁–NC₁₂; see Figure 6. From the computed geometry, $\theta = 49.7^\circ$. The sum of the angles around the nitrogen atom is 342°, clearly smaller than the 360° to be expected for a planar sp² N atom, which is a clear indication of a pronounced pyramidal character. This conclusion is supported by the value of 40° calculated for the pyramidal angle ϕ , defined by the angle between the C₁N bond and the C₁₁NC₁₂ plane (Figure 7).

The lowest harmonic vibrational frequency calculated for the ground state of 1DMAN and 4CIDMAN has a value of 77 and 71 cm⁻¹, respectively. This vibration corresponds to the torsion

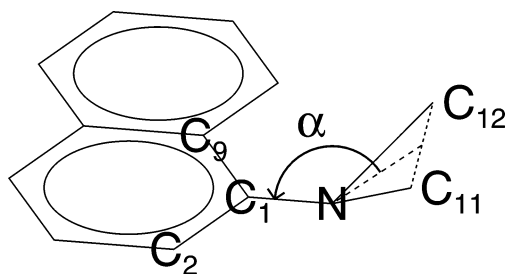


Figure 7. Definitions of the twist and pyramidal angles used in the present study. The twist angle $\theta = (\tau_1 + \tau_2)/2$ where τ_1 and τ_2 are respectively the two dihedral angles $C_2C_1NC_{11}$ and $C_9C_1NC_{12}$. The pyramidal angle Φ is defined as $\Phi = \pi - \alpha$ where α is the angle between the C_1N bond and the line bisecting the $C_{11}NC_{12}$ angle.

of the dimethylamino group around the C_1-N bond and its calculated energy compares quite well with the low frequency observed in the FES spectra (75 cm^{-1}); see Figures 1 and 4.

Torsional Hamiltonian for 4CIDMAN. 4CIDMAN is assumed to consist of two rigid parts, the $N(\text{CH}_3)_2$ group and the chloronaphthalene moiety, as illustrated in Figure 6. The large amplitude coordinate targeted in the present investigation is the twist angle θ of the $N(\text{CH}_3)_2$ group relative to the chloronaphthalene plane, as defined above. $\theta = 90^\circ$ when the molecule has a plane of symmetry, the two methyl groups pointing away on both sides of the naphthalene ring, and $\theta = 0^\circ$ when $\tau_1 = -\tau_2$. With these assumptions, the Hamiltonian corresponding to the internal rotation of the $N(\text{CH}_3)_2$ group in 4CIDMAN is given by²⁰

$$H = FP_\theta^2 + V(\theta) \quad (2)$$

where $F = \hbar/4\pi I_m c$ is the reduced rotational constant of the $N(\text{CH}_3)_2$ group around the $C-N$ bond and I_m is the reduced moment of inertia. P_θ is the conjugate momentum for the θ coordinate and $V(\theta)$ is the torsional potential energy function. It is assumed that the rotational constant F in the Hamiltonian (eq 2) has the same value for the ground state S_0 as for the first excited singlet state S_1 . The ab initio geometry leads to $F = 0.333\text{ cm}^{-1}$ (Figure 6). Eigenvalues and eigenfunctions of the Hamiltonian presented by eq 2 can easily be constructed with the help of a basis set consisting of free rotor functions,²⁰ provided that the potential energy function $V(\theta)$ is expanded as a Fourier series, which is the case in the present investigation.

Potential Energy Functions and Franck-Condon Fitting. For the potential energy function of the ground state S_0 and the excited state S_1 the following expression is employed^{20,21}

$$V(\theta) = (V_1/2)[1 - \cos(\pi/2 - \theta)] + (V_2/2)\{1 - \cos[2(\pi/2 - \theta)]\} \quad (3)$$

where V_1 and V_2 are constants. This choice for $V(\theta)$ ensures that the potential energy function is unchanged by the symmetry operation $\theta \rightarrow \pi - \theta$, corresponding to the symmetry plane of the molecule. The parameters V_1 and V_2 (eq 3) for the electronic ground state S_0 are deduced from the ab initio molecular geometry of 4CIDMAN (Figure 6), which gives an equilibrium value for the amino twist angle θ_{eq} of 49.7° and a harmonic frequency of 71 cm^{-1} for the torsional mode.

According to these data, the following results are obtained for 4CIDMAN: $V_1 = 28\,676\text{ cm}^{-1}$ and $V_2 = -9427\text{ cm}^{-1}$ and a barrier of 541 cm^{-1} for a perpendicular amino group (full twist, $\theta = 90^\circ$). For the excited electronic state S_1 , V_1 and V_2 were derived from the LIF spectrum (Figure 4) by fitting the experimental torsional band positions and intensities according

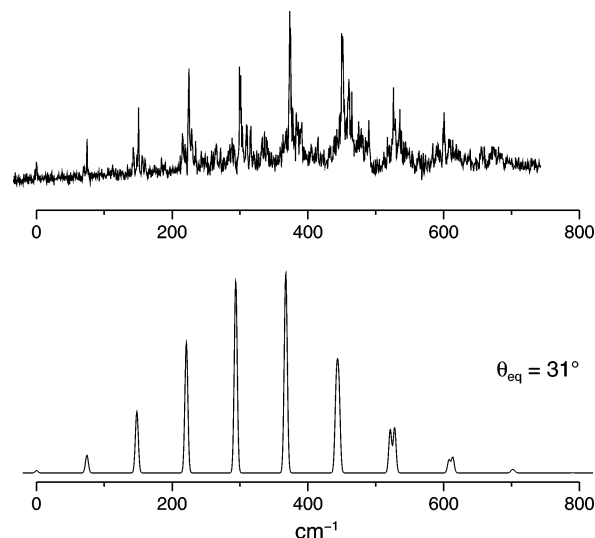


Figure 8. Comparison between the observed and calculated torsional progressions for 4-chloro-1-(dimethylamino)naphthalene (4CIDMAN). The calculated progressions correspond to an equilibrium twist angle θ_{eq} of 31° .

to the Franck-Condon principle. As pointed out in similar treatments,^{21,22} the line positions alone are by themselves not sufficient for an unambiguous determination of the torsional potential energy function, because the torsional energies depend mainly on the shape near the minimum of the potential energy surface and not primarily on the value of θ_{eq} . To determine the value for θ_{eq} , the intensities of the torsional progression bands were computed by calculating the Franck-Condon overlap. The best agreement between the observed and calculated torsional progression (Figure 8) was obtained for $\theta_{\text{eq}} = 31^\circ$ and a barrier of 1349 cm^{-1} , which corresponds to $V_1 = 11\,820\text{ cm}^{-1}$ and $V_2 = -5737\text{ cm}^{-1}$.

The calculated torsional progression is shown in Figure 8, and the corresponding torsional potential energy functions for S_0 and S_1 are plotted in Figure 9. In agreement with the symmetry of the molecule 4CIDMAN, which implies double minima potentials, the torsional levels are identified with a vibrational quantum number ν and with the superscript + or -, which identifies the two tunneling sublevels, thereby indicating whether the torsional functions are symmetric or antisymmetric with respect to the symmetry operation $\theta \rightarrow \pi - \theta$. With the values so obtained for V_1 and V_2 , all observed torsional levels have energies below the potential barrier at $\theta = 90^\circ$. For the S_0 state, the lower $\nu = 0^+$ and $\nu = 0^-$ levels are degenerate within 0.01 cm^{-1} . For the S_1 state, the tunneling doubling is of the order of 10 cm^{-1} for the highest observed torsional levels. Because of the selection rules $+\leftrightarrow +$ and $-\leftrightarrow -$, this gives rise to a splitting of the lines, which can be seen in the calculated progression in Figure 8. This, together with the vibronic coupling with other modes, explains the increased complexity of the spectrum of 4CIDMAN.

In conclusion, the estimated decrease in the equilibrium value of the amino twist angle θ of 18.7° (from 49.7 to 31°) taking place upon S_0-S_1 excitation (see Figure 8) indicates that the (dimethylamino)naphthalenes 1DMAN, 4MDMAN, and 4CIDMAN cannot adopt a totally planar geometry in S_1 , because of the steric hindrance caused by the peri effect between the amino group and the H8 atom of naphthalene, as already discussed above.¹⁵

Nonradiative Deactivation Channel in 1DMAN, 4MDMAN, and 4CIDMAN. One of the most intriguing results of this study is the finding of a dramatic drop of the fluorescence intensity

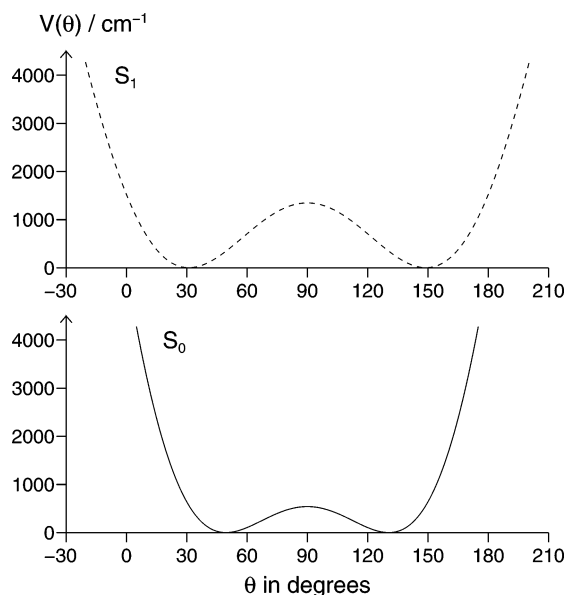


Figure 9. Torsional potential energy functions of 4CIDMAN in its S_0 and S_1 electronic states. The equilibrium amino twist angle θ_{eq} is 49.7° in S_0 and decreases to 31° upon excitation to S_1 . The calculated barrier heights at the perpendicular conformation of the amino group ($\theta = 90^\circ$), are equal to 541 and 1349 cm^{-1} for the S_0 and S_1 states, respectively.

in the excitation spectrum of 1DMAN, with a threshold at an excess energy of about 1000 cm^{-1} (11.9 kJ/mol); see Figure 1. This phenomenon indicates that an energy dependent fast nonradiative pathway occurs, competing with the fluorescence decay from the S_1 state. Simultaneous with the sharp decrease in fluorescence intensity, the excitation spectrum exhibits a series of broad bands (Figure 1), which are the signature of a significant coupling between two electronic states, taking place in this energy region. This behavior can be related to the thermally activated nonradiative process that has been established in solution and which has been attributed to internal conversion (IC), on the basis of fluorescence lifetimes and quantum yield measurements.^{8–11} The proposed mechanism for this thermally activated IC involves the so-called proximity effect²³ between the S_1 and S_2 states and is thus correlated with the energy gap $\Delta E(S_1, S_2)$. According to this description, the vibronic coupling between the two close lying lowest excited singlet states, together with the displacement of the equilibrium geometry along the torsional coordinate in the excited state, flatten the PES and favor the crossing toward the ground state through a conical intersection.¹⁰ The excitation spectra of 1DMAN support the presence of two nearly isoenergetic excited states, together with the activity of the torsional mode along the C–N bond. It should be stressed, however, that the out-of-plane torsional progression, which reveals a large change relative to S_0 of the excited-state potential energy surface along this coordinate, may for symmetry reasons not be the promoting mode for the observed internal conversion.²³ In fact, because both transition moments are in the plane of the naphthalene nucleus, the two lowest singlet excited states of L_a and L_b character are not expected to couple through the out-of-plane modes. For nonplanar geometries, however, the CT states may be involved in the vibronic coupling between the two states, thereby allowing a conical intersection toward the S_0 state to take place at large torsional angles.

The decrease of the fluorescence intensity at higher excitation energies is also observed in the case of the 4-substituted 1DMAN derivatives 4MDMAN and 4CIDMAN and reveals by

its presence that the occurrence of an energy dependent nonradiative process is a general phenomenon in these molecules. The energy thresholds for the nonradiative pathway can be estimated at 1200 cm^{-1} (14.3 kJ/mol) for 4MDMAN and 700 cm^{-1} (8.4 kJ/mol) for 4CIDMAN; see Figures 4 and 7. Also with these molecules, the thresholds determined in the isolated gas phase (although lower than in solution)¹¹ parallel the activation energy found in solution and the thresholds decrease in the order CH_3 , H, Cl for the 4-substituent.

Because the twisting properties of the $\text{N}(\text{CH}_3)_2$ group in 4MDMAN and 4CIDMAN are not influenced by the presence of the substituent in the 4-position (see above), this experimental finding indicates that the curve crossing responsible for the internal conversion process has a barrier that decreases with increasing electron affinity of the 4-substituent in the naphthalene moiety and can hence be related to a larger admixture of states with intramolecular charge-transfer character (ICT) in the lowest excited states.^{3,4}

The effect of complexation of 1DMAN with CH_3CN presents also strong similarities with the behavior observed in solution.^{8–11} The threshold for the nonradiative decay has increased to 1500 cm^{-1} , as compared with bare 1DMAN (1000 cm^{-1}). Besides, the fluorescence decay times of the 1DMAN/ CH_3CN complex have become longer and the fluorescence quantum yield is larger than for uncomplexed 1DMAN as shown by the strong enhancement of the fluorescence excitation spectrum intensity (Figure 5). It should further be noted that the global Franck–Condon envelope of the excitation spectrum observed for the bare molecule is maintained in the complex. One can therefore conclude that the 1DMAN molecule undergoes a similar decrease of the dimethylamino twist angle upon excitation whether complexed with CH_3CN or not.

The solvent dependence of the photophysics of 1DMAN has been explained previously in terms of the mechanism described above.^{8–11} The $S_1(L_a)$ state, which bears some charge-transfer character from the dimethylamino lone pair to the naphthalene π^* orbitals, is stabilized by dipole–dipole interactions with the solvent, whereas the effect on the L_b state is expected to be relatively small. As a result, the coupling between the two states is reduced and this decoupling affects the barrier for the IC process, which becomes larger in acetonitrile (31 kJ/mol) than in *n*-hexane (18 kJ/mol).¹⁰ Although new competitive decay channels that may be responsible for the drop of fluorescence, can be opened in van der Waals complexes at high excess energy, the behavior observed for the bare and complexed 1DMAN can be described according to the same mechanism in the gas phase as in solution. The threshold for the disappearance of fluorescence intensity from the 1DMAN/acetonitrile complex takes place at about 1500 cm^{-1} (18 kJ/mol) above the onset of the spectrum whereas its value is 1000 cm^{-1} (10.9 kJ/mol) in the case of the bare molecule.

Conclusion

The spectroscopic properties of the isolated jet-cooled 1-aminonaphthalenes 1AN, 1MAN, 1DMAN, 4MDMAN, and 4CIDMAN are in accordance with the photophysical behavior of these molecules in solution. The twisted dimethylamino derivatives 1DMAN, 4MDMAN, and 4CIDMAN undergo a large change of their equilibrium geometry upon excitation to S_1 , consisting of an antitwist motion of the amino group toward planarity. The Franck–Condon analysis of the torsional motion in the 4-substituted molecules 4MDMAN and 4CIDMAN indicates that a decrease of about 20° (from 49.7° to 31°) of the amino twist angle takes place upon excitation from S_0 to S_1 . The

molecules undergo a fast nonradiative process in the excited state at higher excess excitation energies, above 1000 cm⁻¹ in the case of IDMAN, which process parallels the thermally activated internal conversion observed with the 1-(dimethyl-amino)naphthalenes in solution.

Acknowledgment. We are greatly indebted to Michel Broquier, who performed part of the ab initio calculations.

References and Notes

- (1) Platt, J. R. *J. Chem. Phys.* **1949**, *17*, 484. Salem, L. *The Molecular Orbital Theory of Conjugated Systems*; Benjamin: New York, 1966.
- (2) Craig, D. P.; Hollas, J. M.; Redies M. F.; Wait, S. C. *Philos. Trans. R. Soc. (London)* **1961**, *253A*, 543.
- (3) Suzuki, S.; Fujii, T.; Baba, H. *J. Mol. Spectrosc.* **1973**, *47*, 243.
- (4) Suzuki, S.; Fujii, T.; Baba, H. *J. Mol. Spectrosc.* **1975**, *57*, 490.
- (5) Berden, G.; Meerts, W. L.; Plusquellic, D. F.; Fujita, I.; Pratt, D. W. *J. Chem. Phys.* **1995**, *104*, 3935.
- (6) Jaffé, H. H.; Orchin, M. *Theory and Applications of Ultraviolet Spectra*; Wiley: New York, 1964.
- (7) Meech, S. R.; O'Connor, R. V.; Phillips, D.; Lee, A. G. *J. Chem. Soc., Faraday Trans.* **1983**, *79*, 1563.
- (8) Zachariasse, K. A.; Grobys, M.; von der Haar, Th.; Hebecker, A.; Il'ichev, V.; Yu, V.; Jiang, Y. B.; Morawski, O.; Ruckert, I.; Kühnle, W. *J. Photochem. Photobiol. A: Chem.* **1997**, *105*, 373.
- (9) Suzuki, K.; Tanabe, H.; Tobita S.; Shizuka, H. *J. Phys. Chem. A* **1997**, *101*, 4496.
- (10) Rückert, I.; Demeter, A.; Morawski, O.; Kühnle, W.; Tauer, E.; Zachariasse, K. A. *J. Phys. Chem. A* **1999**, *103*, 1958.
- (11) Suzuki, K.; Demeter, A.; Kühnle, W.; Tauer, E.; Zachariasse, K. A.; Tobita S.; Shizuka, H. *Phys. Chem. Chem. Phys.* **2000**, *2*, 981.
- (12) Broquier, M.; Lahmani, F.; Zehnacker-Rentien, A.; Brenner, V.; Millié, P.; Peremans, A. *J. Phys. Chem. A* **2001**, *105*, 6841.
- (13) Frisch, M. J.; Trucks, G. W.; Schlegel, H. B.; Scuseria, G. E.; Robb, M. A.; Cheeseman, J. R.; Zakrzewski, V. G.; Montgomery, J. A., Jr.; Stratmann, R. E.; Burant, J. C.; Dapprich, S.; Millam, J. M.; Daniels, A. D.; Kudin, K. N.; Strain, M. C.; Farkas, O.; Tomasi, J.; Barone, V.; Cossi, M.; Cammi, R.; Mennucci, B.; Pomelli, C.; Adamo, C.; Clifford, S.; Ochterski, J.; Petersson, G. A.; Ayala, P. Y.; Cui, Q.; Morokuma, K.; Malick, D. K.; Rabuck, A. D.; Raghavachari, K.; Foresman, J. B.; Cioslowski, J.; Ortiz, J. V.; Stefanov, B. B.; Liu, G.; Liashenko, A.; Piskorz, P.; Komaromi, I.; Gomperts, R.; Martin, R. L.; Fox, D. J.; Keith, T.; Al-Laham, M. A.; Peng, C. Y.; Nanayakkara, A.; Gonzalez, C.; Challacombe, M.; Gill, P. M. W.; Johnson, B. G.; Chen, W.; Wong, M. W.; Andres, J. L.; Head-Gordon, M.; Replogle, E. S.; Pople, J. A. *Gaussian 98*, revision A.6; Gaussian, Inc.: Pittsburgh, PA, 1998.
- (14) Daum, R.; Druzhinin, S.; Ernst, D.; Rupp, L.; Schroeder, J.; Zachariasse, K. A. *Chem. Phys. Lett.* **2001**, *341*, 272.
- (15) Balasubramanian, V. *Chem. Rev.* **1966**, *66*, 567.
- (16) Petruska, J. A. in *Systematics of the Electronic Spectra of Conjugated Molecules: a source book*; Wiley: New York, 1964.
- (17) Birks, J. B. *Photophysics of Aromatic Molecules*; Wiley: London, 1970.
- (18) Jacobson, B. A.; Guest, J. A.; Novak F. A.; Rice, S. A. *J. Chem. Phys.* **1987**, *87*, 269.
- (19) Lakshminarayan, C.; Knee, J. L. *J. Phys. Chem. A* **1990**, *94*, 2637.
- (20) Weersink, R. A.; Wallace, S. C.; Gordon, R. D. *J. Chem. Phys.* **1995**, *103*, 9530.
- (21) Grassian, V. H.; Warren, A.; Bernstein, E. R. *J. Chem. Phys.* **1989**, *90*, 3394.
- (22) Gordon, R. D. *J. Chem. Phys.* **1990**, *93*, 6908.
- (23) Lim, E. C. In *Advances in Photochemistry*; Neckers, D. C.; Volman, D. H.; von Büna, G., Eds.; Wiley: New York, **1997**, *23*, 165.